Self-Consistent Calculations of the Energy Band Structure of Mg_2Si†

NATHAN O. FOLLAND*
Institute for Atomic Research and Department of Physics, Iowa State University, Ames, Iowa
(Received 15 July 1966; revised manuscript received 1 February 1967)

Self-consistent calculations of the band structure of the semiconducting compound Mg_2Si are presented for the nonrelativistic Hartree and Hartree-Fock (HF) independent-particle models (IPM's). The IPM's are based on a finitely periodic model of the many-electron system. Some advantages and distinctions of this model with respect to the conventional formulation are discussed. The calculations are broken into two parts. First-order core (tight-binding) functions and energies are obtained from a model in which all valence effects are neglected. The dominant valence contributions are included in the final stage of calculation where the basis consists of first-order core functions and orthogonalized plane waves. Approximations to matrix elements are described and the error is estimated. The calculations reveal that the valence-band maximum occurs at $\Gamma(\Gamma_{15})$ and the conduction band is many-valleyed with minima at the equivalent points $X(X_3)$. These results agree with qualitative predictions of band symmetries based on experimental charge densities and a symmetry analysis using linear combinations of atomic orbitals. A preliminary investigation indicates that the Hartree bands are in good quantitative agreement with optical data and should be a valuable aid in the interpretation of experiment. The HF-IPM results for Mg_2Si are compared with results for HF calculations in free atoms.

I. INTRODUCTION

THE fundamental concept underlying the band theory of solids is the independent-particle model (IPM) of a crystal.[1] A single electron is pictured in the static averaged field of the remaining electrons and nuclei. An IPM provides a conceptually simple framework for qualitative and quantitative interpretation of the electronic properties of crystalline materials. Since IPM's of a many-electron system usually are based on the Hartree-Fock (HF) approximation,[2] it is important that both the capabilities and limitations of the HF-IPM's be understood. For this reason we have attempted to calculate the nonrelativistic HF electron-energy bands of the semiconducting compound Mg_2Si as accurately and with as few restrictions as practical considerations allowed.

The problem of making a self-consistent (SC) IPM calculation may be stated in three interdependent parts. Firstly, the many-electron Schrödinger equation is obtained and the HF equations derived. Secondly, the representations of the single-particle functions and HF operators are chosen such that SC calculations are possible. Thirdly, the SC calculations are formulated and performed.

As it is convenient to represent a part or all of certain wave functions as a linear combination of plane waves, we first consider the integrals which will occur in the usual form of the HF equations. In the case of matrix elements with the exchange operator, integrals occur which have the form[3]

$$\int \exp[i(\mathbf{k}-\mathbf{k}')\cdot(\mathbf{r}_1-\mathbf{r}_2)]\,(2/r_{12}\Omega_1^2)d\mathbf{r}_1 d\mathbf{r}_2 = (8\pi/\Omega_1)(\mathbf{k}-\mathbf{k}')^{-2}. \quad (1)$$

If $\mathbf{k}=\mathbf{k}'$, this integral diverges. In principle this difficulty can be eliminated[4] by replacing the finitely periodic model crystal by an infinite model crystal. Then $\mathbf{k}$ is a continuous variable and the divergence of Eq. (1) is quadratically integrable.

In this paper the problem is treated by a modification of the formulation of the many-electron problem. A periodicity is imposed on the many-electron system such that the many-electron Hamiltonian displays a finite period. Thus, the electronic and nuclear contributions to the potential energy in the many-electron Hamiltonian may be represented by expansions in plane waves as is customarily done in the theory of the electron gas. In this way the infinities of Eq. (1) are removed while retaining a finitely periodic model crystal.

An important practical advantage is obtained if the number N_0 of translationally inequivalent points in a finitely periodic model can be taken to be small. There are experimental grounds for believing that a model where $N_0^{1/3}\sim 2$ to 4 provides a good description of the electronic problem. Cardona[5] has found essentially identical reflection spectra for zincblende and wurtzite forms of ZnS. Birman[6] noted that with respect to a Zn or S site the first-neighbor shells are identical and the

† Work was performed in the Ames Laboratory of the U. S. Atomic Energy Commission. Contribution No. 1925.
* Present address: Physics Department, Kansas State University, Manhattan, Kansas.
[1] See, e.g., W. Kurtzelnigg and V. Smith, Report No. 130, Quantum Chemistry Group, Uppsala, Sweden (unpublished).
[2] See, e.g., C. C. J. Roothaan, Rev. Mod. Phys. 32, 179 (1960).
[3] See, e.g., J. Callaway, *Energy Band Theory* (Academic Press Inc., New York, 1964), p. 122.
[4] J. Phillips and L. Kleinman [Phys. Rev. 128, 2098 (1962)] evaluate this integral with the aid of an argument in which the divergence is regarded as arising from an inadequate sampling procedure.
[5] M. Cardona and G. Harbeke, in *Proceedings of the Seventh International Conference on the Physics of Semiconductors* (Dunod Cie., Paris, 1964), p. 217.
[6] J. L. Birman, Phys. Rev. 115, 1493 (1959).

second-neighbor shells are very similar in the two crystal structures. Thus the dependence of the electron-energy bands on crystal structure must be largely determined by interactions with the first few neighbors.[7]

In Sec. II the periodically extended crystal model (ECM) is defined. The many-electron Hamiltonian and HF equations are obtained for this model. The formulation of the Mg_2Si calculations is presented in Sec. III. Core functions are represented by tight-binding functions and valence functions by linear combinations of orthogonalized plane waves. Approximations made in forming the HF operators and in calculating the matrix elements are described and the error involved is estimated.

In order to include HF exchange it is essential to the analytic functions and thereby reduce many integrals to simple rational expressions. For this reason it was not feasible to perform calculations based on Slater's $(\rho^{1/3})$ exchange approximation.[8]

The results for SC calculations based on the Hartree and HF IPM's are presented in Sec. IV. Finally, in Sec. V the calculations are reviewed with respect to comparable calculations.

Atomic units (a.u.) are used throughout except that energies are expressed in rydbergs (2 Ry = 1 a.u. = 27.21 eV).

II. THE EXTENDED CRYSTAL MODEL

A. Definition of the Extended Crystal Model

An ideal crystal may be defined with respect to a lattice of points in space. Let $\{\mathbf{a}_i\}$, $i=1, 2, 3$ be a set of linearly independent primitive vectors. The space lattice is the set of points $\{\mathbf{R}\}$ where a particular vector of the set,

$$\mathbf{R}(\mathbf{m})=m_1\mathbf{a}_1+m_2\mathbf{a}_2+m_3\mathbf{a}_3, \tag{2a}$$

is specified by $\mathbf{m}=(m_1,m_2,m_3)$ where the components of $\mathbf{m}$ are natural numbers. The set of points $\{\mathbf{K}\}$ where a member,[9]

$$\mathbf{K}(\mathbf{m})=m_1\mathbf{b}_1+m_2\mathbf{b}_2+m_3\mathbf{b}_3, \tag{2b}$$

is expressed in terms of the vectors $\{\mathbf{b}_i=(2\pi/\Omega_0)\times\epsilon_{ijk}\mathbf{a}_j\times\mathbf{a}_k\}$, $i=1, 2, 3$, $(\Omega_0=\mathbf{a}_1\cdot\mathbf{a}_2\times\mathbf{a}_3)$ has the property that

$$\mathbf{K}(\mathbf{m})\cdot\mathbf{R}(\mathbf{n})=2\pi\mathbf{m}\cdot\mathbf{n}. \tag{3}$$

The lattice formed from the set of points $\{\mathbf{K}\}$ is the lattice reciprocal to the space lattice. The three families of parallel planes,

$$\mathbf{b}_i\cdot\mathbf{r}=2\pi h, \quad i=1, 2, 3, \tag{4}$$

where h is a natural number, partition the space into elementary cells each of which is a parallelepiped of volume Ω_0.

A finite crystal is considered to occupy a parallelepiped in space whose edges are the vectors $\{\mathbf{A}_i=N\mathbf{a}_i\}$, $i=1, 2, 3$. The volume of the finite crystal is $\Omega_1=N^3\Omega_0$. The finite-crystal lattice is the set of points $\{\mathbf{R}^c\}$ where

$$\mathbf{R}^c(\mathbf{m})=m_1\mathbf{A}_1+m_2\mathbf{A}_2+m_3\mathbf{A}_3. \tag{5}$$

The vectors $\{\mathbf{R}^c\}$ will be called finite crystal lattice vectors. The vectors $\{\mathbf{k}\}$ reciprocal to the finite-crystal vectors,

$$\mathbf{k}(\mathbf{m})=m_1\mathbf{B}_1+m_2\mathbf{B}_2+m_3\mathbf{B}_3, \tag{6}$$

where $\{\mathbf{B}_i=(2\pi/\Omega_1)\epsilon_{ijk}\mathbf{A}_j\times\mathbf{A}_k=\mathbf{b}_i/N\}$, $i=1, 2, 3$, will be designated $\mathbf{k}$ vectors. Evidently, $\mathbf{k}(N\mathbf{m})=\mathbf{K}(\mathbf{m})$.

The finite crystal consists of nuclei and atoms which are confined within the crystal volume. The structure of the finite crystal is defined by specifying the equilibrium location and species of nuclei within a prototype elementary cell. Each elementary cell of the finite crystal contains nuclei of the same elements in the same relative position as in every other cell. The nuclei are treated as point particles which are fixed at their equilibrium positions. The number of electrons in the finite crystal is such that the crystal as a whole is electrically neutral.

The periodically extended finite crystal or extended crystal model (ECM) is an infinite crystal. The ECM is defined with respect to the finite crystal lattice. The prototype elementary cell or ECM cell is the finite crystal defined above. Each ECM cell is required to be identical in every respect to the prototype ECM cell. The nuclear charge distribution is periodic in space with periods $\{\mathbf{a}_i\}$, $i=1, 2, 3$, and the electron-charge distribution is periodic in space with periods $\{\mathbf{A}_i\}$, $i=1, 2, 3$. Expectation values of operators are to be averaged over an ECM cell. Wave functions and other functions which represent a property of the ECM many-electron system are required to be periodic with at least the periods $\{\mathbf{A}_i\}$. In particular the many-electron operators are required to be periodic with at least periods $\{\mathbf{A}_i\}$.

The ECM is so defined that points in space which are related by a finite crystal lattice vector are equivalent. That is, ECM functions must transform according to the identity representation of the (infinite-order) subgroup T_{fc} of the translation group consisting of transformations by finite crystal lattice vectors. Therefore, the only representations of the (infinite-order) translation group T which occur in the ECM are those of the factor group T/T_{fc}. The order of this factor group is N_0, the number of lattice points in an ECM cell. Each element of the factor group is a set of translations which differ at most by a finite crystal lattice vector. Thus, only a representative translation from a factor group element is needed to describe the element. These

[7] Professor F. Bassani pointed out the significance of the ZnS reflection measurements (private communication).

[8] J. C. Slater, Phys. Rev. **81**, 385 (1951).

[9] Usually when treating lattice vectors or their reciprocals, the entire set is considered. For this reason we adopt the notation where $\mathbf{R}$ (or $\mathbf{K}$, etc.) refers to any member of the set. Thus, $\sum_{\mathbf{K}}$ indicates a sum over all $\mathbf{K}$ vectors. If a particular vector is considered, a subscript is added [e.g., $\mathbf{R}(\mathbf{n})$ or $\mathbf{K}(\mathbf{m})$].

representative translations may be chosen to correspond to the lattice vectors in the prototype ECM cell.[10]

B. The ECM Many-Electron Hamiltonian

The first step toward obtaining the ECM many-electron Hamiltonian is the derivation of the potential due to the ECM charge distribution. The potentials due to nuclear and electronic charges will each be required to satisfy the following conditions:

$$(1) \quad -\nabla^2\varphi(\mathbf{r})=8\pi\rho(\mathbf{r}), \tag{7a}$$

$$(2) \quad \varphi(\mathbf{r}+\mathbf{R}^c)=\varphi(\mathbf{r}), \tag{7b}$$

$$(3) \quad \int_{\mathrm{ECM}} \varphi(\mathbf{r})d\mathbf{r}=0. \tag{7c}$$

The first condition requires φ to be a solution of Poisson's equation. The remaining conditions require φ to be periodic in the finite crystal lattice and average to zero over an ECM cell. The three conditions completely specify the potentials if the charge density is known.

It is convenient to expand potentials in terms of the potential produced by a standard charge density. In each ECM cell this standard charge density consists of a delta function of unit magnitude at the point $\mathbf{r}'$ and a neutralizing uniform charge density:

$$\rho_0(\mathbf{r})=\sum_{\mathbf{R}^c}[\delta(\mathbf{r}-\mathbf{r}'-\mathbf{R}^c)-\Omega_1^{-1}] \tag{8}$$

$$=\sum_{\mathbf{k}\neq 0}\Omega_1^{-1}\exp[i\mathbf{k}\cdot(\mathbf{r}-\mathbf{r}')]. \tag{9}$$

The corresponding potential at the point $\mathbf{r}$ that satisfies conditions (7) is

$$\varphi_0(\mathbf{r}-\mathbf{r}')=\sum_{\mathbf{k}\neq 0}(8\pi/k^2\Omega_1)\exp[i\mathbf{k}\cdot(\mathbf{r}-\mathbf{r}')]. \tag{10}$$

The potential-energy contribution to the many-electron Hamiltonian for a single ECM cell consists of the potential energy due to the interaction of the electrons in the cell with all the other charges, electronic and nuclear, in the extended crystal. The many-electron Hamiltonian is

$$H_e=\sum_i T_i+\sum_i H_i+\tfrac{1}{2}\sum_{i\neq j}H_{ij}, \tag{11}$$

where $T_i=-\nabla^2_i$ is the kinetic-energy operator for electron i and H_i represents the potential energy due to the interaction of electron i with the nuclear charges Z_s at positions $\mathbf{R}_s$ in the elementary cell associated with a space lattice vector $\mathbf{R}$,

$$H_i=-\sum_{\mathbf{R}}\sum_s Z_s\varphi_0(\mathbf{r}_i-\mathbf{R}-\mathbf{R}_s), \tag{12a}$$

where φ_0 is given by Eq. (10). After the sum on $\mathbf{R}$ is evaluated, Eq. (12a) becomes

$$H_i=-\sum_{\mathbf{K}\neq 0}\sum_s Z_s(8\pi/K^2\Omega_0)\exp[i\mathbf{K}\cdot(\mathbf{r}_i-\mathbf{R}_s)]. \tag{12b}$$

The potential due to electron-electron interactions is

$$H_{ij}=\varphi_0(\mathbf{r}_i-\mathbf{r}_j). \tag{13}$$

The factor $\frac{1}{2}$ on the electron-electron interaction term of Eq. (11) assures that these potential-energy contributions are not counted twice.

C. Single-Particle Equations

The HF equations are obtained in the usual way.[2] In the case of paired spin states the HF equations are

$$H_{\mathrm{HF}}u_i=\epsilon_i u_i, \tag{14a}$$

where the HF operator is given in terms of a direct operator D and an exchange operator A by

$$H_{\mathrm{HF}}(1)=T_1+H_1+D_1+A_1. \tag{14b}$$

The direct term is

$$D_1u_i(1)=\sum_j(u_j(2);H_{12}u_j(2))u_i(1), \tag{14c}$$

and the exchange term is

$$A_1u_i(1)=-\sum_j(u_j(2);H_{12}u_i(2))u_j(1). \tag{14d}$$

The eigenfunctions of the ground-state HF operator corresponding to unoccupied single-particle states represent excited states of the many-electron system in the sense of Koopmans's theorem.[11]

In the HF Eqs. (14) the Coulomb interaction potential H_{12} is given by Eqs. (13) and (10). So, for this model the integrals corresponding to Eq. (1) are zero if $\mathbf{k}=\mathbf{k}'$ and no divergence occurs. Thus, for a specific choice of finite ECM cell the corresponding finite set of inequivalent points in the Brillouin zone completely specify the model and in this sense are not just a conveniently chosen but arbitrary sampling of the Brillouin zone.

It is evident that periodic boundary conditions imposed on the finite-crystal HF equations involve more than a periodicity requirement on the single-particle wave functions. There seem to be two alternatives. (1) Let the crystal become infinite. Then periodic boundary conditions are no more than a device to facilitate the discussion of translation symmetry. (2) If the periodicity imposed is to be truly finite, the HF equations must be symmetrized. In particular, the nuclear term must be made compatible with periodicity conditions. Thus, the ECM may be considered a means to effect the symmetrization of the HF equations for a finitely periodic model. We note that in the limit of

[10] A sum on lattice vectors $\sum_{\mathbf{R}}$ in the ECM will include only the N_0 inequivalent vectors contained in the prototype ECM cell.

[11] T. Koopmans, Physica 1, 104 (1933).

infinite ECM cell volume, the ECM-HF model is identical with the infinite-crystal model.

For many purposes a plane-wave expansion of the Coulomb potential is not a convenient form. Alternative forms for the Coulomb interaction may be obtained by the standard methods employed for lattice sums. In Appendix A a simple generalized[17] method is used to obtain the Ewald form and an alternative form of the Coulomb interaction in a periodically extended crystal.

III. CALCULATION OF THE ENERGY BANDS FOR Mg_2Si

A. Physical Properties of Mg_2Si

The crystal structure of Mg_2Si was first determined by Owen and Preston.[12] Their x-ray diffraction experiments showed that the Si atoms form a fcc lattice with lattice constant $a=6.391$ Å. Relative to each Si atom are 8 Mg atoms located at the points $(\pm\frac{1}{4}, \pm\frac{1}{4}, \pm\frac{1}{4})a$. The Mg atoms form a simple cubic lattice with lattice constant $a/2$. The position of the atoms in a unit cell is shown in Fig. 1. The crystal structure just described is called the antifluorite structure. The space group is $Fm3m$ (O_h^5) and the point group with respect to a Si center of symmetry is the full cubic group $m3m$ (O_h). Since the space lattice is fcc, the reciprocal lattice is bcc. Reduced **k** vectors of special symmetry are labeled according to the notation of Bouckaert *et al.*[13]

More recent investigations[14] of the crystal structure of Mg_2Si have shown the lattice constant to be $a=6.338$ Å. Ageev and Guseva[14] calculated the electron-density distributions from their x-ray diffraction data. A reproduction of their results is shown graphically in Fig. 2 where the electron-density distribution is plotted from a Si site along the lines (100), (110), and (111) and from a Mg site along the line (001). The atomic sites are labeled A, B, etc., to correspond to Fig. 1.

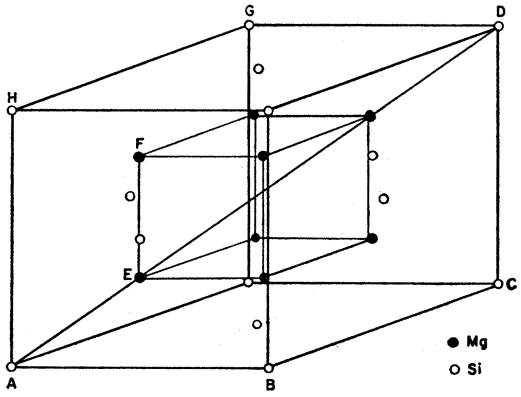

FIG. 1. The position of Mg and Si atoms in the basic cube.

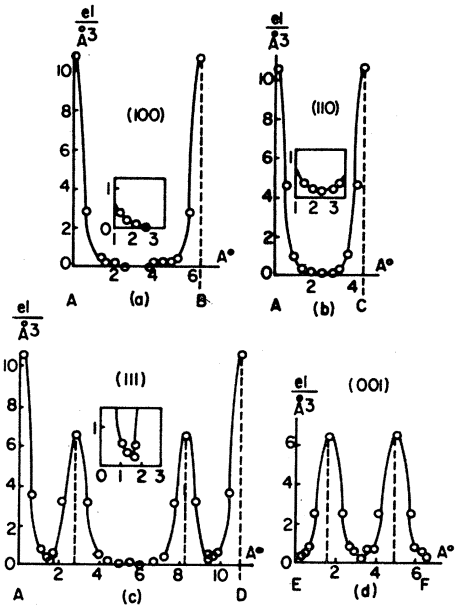

FIG. 2. Electron-density distributions for Mg_2Si in the directions: (a) [100], (b) [110], (c) [111], (d) [001]. From Ageev and Guseva (Ref. 14).

The electron density in the neighborhood of a Si site is observed to be nearly spherically symmetric about the Si site. The electron density about a Mg site exhibits a sizable distortion from spherical symmetry. An estimate of the ionicity of the atomic constituents was obtained by calculating the number of electrons near the Si and Mg sites from a spherical approximation to the Ageev and Guseva charge density. This admittedly rough estimate accounted for 10 of the 12 Mg electrons and all 14 of the Si electrons. From Ageev and Guseva's quotation (0.2 electrons/Å^3) of the charge density in the region of the Si-Si bond it appears that at least one of the remaining electrons is involved in the Si-Si bond. Presumably the one remaining electron is shared by the Si and Mg atoms in the Si-Mg bond. However, this conclusion should not be taken too seriously since Ageev and Guseva pointedly refuse to estimate the ionicity. They argue that the absence of a sharp boundary between the separate ions makes an estimate of the ionicity impossible. This is probably the most realistic estimate of the situation. From the Mg binding energy in Mg_2Si, Whitten[15] estimates an upper limit for the Mg ionicity to be 0.66 electrons. One can obtain this result by assuming that the 2 electrons in the Si-Mg bond are shared on a $\frac{1}{3}$–$\frac{2}{3}$ basis.[16] Although the extent of the ionic character of the Mg atom is not determined, it is clear that a self-consistent calculation of the electronic energy levels must be sufficiently flexible to allow for charge transfer from a Mg to a Si

[12] E. A. Owen and G. D. Preston, Proc. Phys. Soc. (London) **36**, 343 (1924).
[13] L. P. Bouckaert, R. Smoluchowski, and E. Wigner, Phys. Rev. **50**, 58 (1936).
[14] N. V. Ageev and L. N. Guseva, Bull. Acad. Sci. USSR, Div. Chem. Sci. **1**, 31 (1952).
[15] W. B. Whitten, P. L. Chung, and G. C. Danielson, J. Phys. Chem. Solids **26**, 49 (1965).
[16] L. A. Lott and D. W. Lynch, Phys. Rev. **141**, 681 (1966).

TABLE I. Symmetry species which occur in LCAO's formed from Mg and Si s and p orbitals at Γ, X, L.

LCAO	Symmetry species Γ	X	L
Si s	Γ_1	X_1	L_1
Si p	Γ_{15}	$X_{4'}$, $X_{5'}$	$L_{2'}$, $L_{3'}$
Mg^+ s	Γ_1	X_3	L_1
Mg^- s	$\Gamma_{2'}$	$X_{4'}$	$L_{2'}$
Mg^+ p	Γ_{15}	$X_{2'}$, X_5	$L_{2'}$, $L_{3'}$
Mg^- p	$\Gamma_{25'}$	X_1, X_5	L_1, L_3

atom and to include the effects of the unscreened Mg nucleus.

Mg_2Si is a semiconductor. The energy gap has been determined both electrically and optically. The results from the various measurements of the energy gap have been summarized and discussed by Stella.[17] The electrical gap is 0.77 eV, the optical gap is about 0.67 eV and the photoconductive gap is 0.65 eV at 15°K. Reflectivity measurements by Scouler[18] indicated that the direct gap is about 2.1 eV.

B. Preliminary Investigation of the Band Symmetries

The probable symmetries of the valence bands and low-lying conduction levels may be predicted for the points Γ, X, L by considering the dominant terms which would occur in a LCAO (linear combination of atomic orbitals) calculation of these energy levels. For this purpose LCAO's formed from the $3s$ and $3p$ atomic orbitals will be considered. In the case of Mg, symmetry-adapted LCAO's formed from s and p functions centered about Mg sites consist of symmetric (Mg^+) and antisymmetric (Mg^-) combinations of the Mg orbitals centered about the two Mg sites in an elementary cell. In Table I are listed the symmetry species of the Mg and Si LCAO's for the points Γ, X, L.

From the charge-density results, we expect the valence functions to be dominated by Si LCAO's. Thus, the valence symmetries will be those of the Si s and p LCAO's in Table I. This choice for the valence symmetries is consistent with the semiconducting property of Mg_2Si and at Γ and L is the only reasonable choice that can be made.

It is likely that the low-lying conduction levels at Γ will be Γ_1 and Γ_2, since the mixing between the Si and Mg Γ_1 functions is not likely to be large and the Mg p levels must lie above the s levels as in the free atom. However, a quantitative argument must be used to determine the order of the Γ_1 and $\Gamma_{2'}$ conduction levels.

At L the mixing between the Mg $L_{2'}$ and the Si $L_{2'}$ LCAO's may be quite strong, suggesting that the $L_{2'}$ valence level will lie appreciably below the $L_{3'}$ valence level. Within this scheme there are two choices for the low-lying conduction level at L, L_1, and $L_{2'}$. Since the L_1 mixing must be about the same as the Γ_1 mixing, the L_1 and Γ_1 conduction levels should be at about the same position. Because of the additional $L_{2'}$ mixing with the Si p function at L the $L_{2'}$ level will lie above the $\Gamma_{2'}$ level.

At X the candidates for the low-lying conduction levels are $X_{4'}$ and X_3. Since the Si $X_{4'}$ LCAO mixes with the Mg LCAO of this symmetry, the low-lying conduction level at X must be X_3. Since there is no mixing with the valence levels, it appears that the X_3 level is the bottom of the conduction band. This is consistent with Whitten's prediction[19] from measurements of piezoelectric effect that the conduction band minimum occurs in the [100] direction.

C. Formulation of the SC Calculations

1. *The Bare-Ion Model for the Core Functions*

In SC calculations the HF operator itself is unknown. A zeroth-order approximation to the HF operator is made. The solutions of this problem are obtained and then used to form an improved HF operator. Thus, it is essential that the formulation of the calculation be flexible enough so that the SC iterative procedure is practicable. Such a scheme is described in the following paragraphs.

In the region about a nuclear site the Coulombic attraction of the nuclear charge will be the dominant factor governing the distribution of the electronic probability density. The wave function (core function) for an electron whose probability density lies predominantly in the vicinity of a nuclear site should closely resemble the corresponding free atom or free ion wave function in this region. Thus, the wave function in the crystal should be well-described by a single LCAO or linear combination of a small number of LCAO's formed from the low-lying atomic wave functions (orbitals). Core LCAO's are defined to be single LCAO's formed from those atomic orbitals (core orbitals) which when centered about different nuclear sites in the crystal overlap negligibly with one another.

In the bare-ion model for the core electrons a first approximation is obtained for the core functions and eigenvalues. In this model all effects due to occupied noncore (valence) orbitals are neglected. The dominant effects of the valence electrons on core electrons are included self-consistently or estimated in the next stage of calculations.

The zeroth-order HF operator for the bare-ion model is formed from core LCAO's,

$$H_{\mathrm{HF}}^{\mathrm{BI}} \approx -\nabla^2 + V_{\mathrm{core}} + A_{\mathrm{core}}, \qquad (15)$$

[17] A. Stella and D. W. Lynch, J. Phys. Chem. Solids 25, 1253 (1964).

[18] W. J. Scouler, Lincoln Laboratories, Lexington, Massachusetts. Reflectivity data, 1965 (private communication).

[19] W. B. Whitten and G. C. Danielson, in *Proceedings of the Seventh International Conference on the Physics of Semiconductors* (Dunod Cie., Paris, 1964), p. 537.

where A_{core} is the core-exchange operator,

$$A_{\text{core}}\phi(\mathbf{r})=-\sum_{js,\mathbf{R}}\int\phi_{js}^{*}(\mathbf{r}'-\mathbf{R}-\mathbf{R}_s)H_{12}\phi(\mathbf{r}')d\mathbf{r}' \times\phi_{js}(\mathbf{r}-\mathbf{R}-\mathbf{R}_s), \quad (16)$$

written in terms of core orbitals of type j centered about a nuclear site s. The plane-wave expansion of the direct term V_{core} is

$$V_{\text{core}}=\sum_{\mathbf{K}\neq 0}(8\pi/K^2\Omega_0)\rho_{\mathbf{K}}\exp(i\mathbf{K}\cdot\mathbf{r}), \quad (17a)$$

where

$$\rho_{\mathbf{K}}=\sum_s\exp(-i\mathbf{K}\cdot\mathbf{R}_s)\left[-Z_s+2\sum_j\int|\phi_{js}(\mathbf{x})|^2 \times\exp(-i\mathbf{K}\cdot\mathbf{x})d\mathbf{x}\right]. \quad (17b)$$

It is easy to show that Eqs. (17) are equivalent to

$$V_{\text{core}}=\sum_{s,\mathbf{R}}V_s(\mathbf{r}-\mathbf{R}-\mathbf{R}_s)+H_{\text{ion}}-V_0, \quad (18a)$$

where each V_s is an atomiclike potential which includes the potential due to the Z_s' core electrons and Z_s' nuclear charges associated with nuclear site s,

$$V_s(\mathbf{r}_1)=-2Z_s'/r_1+4\sum_j\int|\phi_{js}(\mathbf{r}_2)|^2r_{12}^{-1}d\mathbf{r}_2. \quad (18b)$$

The potential due to the remaining nuclear charges ($Z_s^{\text{ion}}=Z_s-Z_s'$) is included in

$$H_{\text{ion}}=\sum_{\mathbf{K}\neq 0}V_{\mathbf{K}}^{\text{ion}}\exp(i\mathbf{K}\cdot\mathbf{r}), \quad (18c)$$

with

$$V_{\mathbf{K}}^{\text{ion}}=\sum_s-Z_s^{\text{ion}}(8\pi/K^2\Omega_0)\exp(-i\mathbf{K}\cdot\mathbf{R}_s). \quad (18d)$$

The term V_0,

$$\Omega_0V_0=\sum_s\int V_s(\mathbf{x})d\mathbf{x} =-(8\pi/3)\sum_{s,j}\int|\phi_{js}(\mathbf{r})|^2r^2d\mathbf{r}, \quad (18e)$$

must be included so that the average value of the potential is zero.

In Mg_2Si the closed-shell orbitals corresponding to doubly ionized Mg and 4-times ionized Si are regarded as defining the cores. Thus, $Z_{\text{Mg}}^{\text{ion}}=2$ and $Z_{\text{Si}}^{\text{ion}}=4$. The dominant behavior of the ion term near site s is

$$H_{\text{ion}}\approx-2Z_s^{\text{ion}}/r_s+V_s^{\text{shift}}, \quad (19)$$

where V_s^{shift} is the Madelung shift associated with atom s. The Madelung shifts for the Mg and Si sites are 2.4038 Ry and 3.598 Ry, respectively. The shifts quoted above were calculated from tables prepared by Slater and DeCicco.[20]

In the vicinity of a nuclear site the bare-ion HF operator is very nearly a free ion HF operator. The eigenfunctions are approximated by single LCAO's formed from the free ion atomic orbitals. The eigenvalues are shifted from their atomic values by the Madelung shifts and V_0.

Equation (19) is an approximation to the ionic term which is strictly valid only at the nuclear site. A numerical investigation of the behavior of this term indicates that the core eigenvalues calculated in this approximation will be within 0.2 Ry of the exact value. An attempt was made to incorporate the ionic correction into the bare-ion calculation exactly. The ionic potential was written as an Ewald sum (see Appendix A) where the Ewald parameter was chosen to emphasize the plane-wave series. The heavily screened lattice-sum terms from the neighboring sites were neglected. Owing to this error the method failed, because the results were not clearly independent of the Ewald parameter. However, it was evident from this calculation that the effect of the ionic potential on the bare-ion core *functions* is negligible and that the bare-ion core *eigenvalues* are shifted by nearly a constant (the $2p$ and $2s$ eigenvalues were shifted slightly more than the $1s$ eigenvalue). Since the Madelung shift is an approximation, the sensitivity of the noncore eigenvalues to small shifts of the core eigenvalues will be studied in the next stage of calculation.

2. *Approximations in the Matrix Elements*

In the crystal calculation all eigenfunctions are expanded in a basis set consisting of symmetry-adapted bare-ion core functions,

$$H_{\text{HF}}^{\text{BI}}\psi_c=E_c\psi_c, \quad (20)$$

augmented by symmetry-adapted plane waves (SPW's) formed from about 65 plane waves. The SPW's are orthogonalized to the core functions to form symmetry-adapted orthogonalized plane waves (SOPW's),

$$\text{SOPW},\mathbf{k})=\text{SPW},\mathbf{k})-\sum_c(\psi_c;\text{SPW},\mathbf{k})\psi_c. \quad (21)$$

The HF operator in the crystal is partitioned into a bare-ion term, a term which reflects changes in the core functions and a valence term,

$$H_{\text{HF}}=H_{\text{HF}}^{\text{BI}}+H_{\text{HF}}^{\text{core}}+H_{\text{HF}}^{\text{val}}. \quad (22a)$$

Two approximations are made in forming the HF operator. The first is to neglect the changes in the core-exchange operator. The second is to approximate the valence functions in the valence-exchange operator by a truncated series of SPW's.

The effect of the valence terms on the bare-ion core

[20] J. C. Slater and P. DeCicco, Solid State and Molecular Theory Group, M.I.T. Quarterly Progress Report No. 50, p. 46 (unpublished).

functions should be comparable to the corresponding effect in the free atom or ion. To estimate the magnitude of the effect, the Mg and Si neutral-atom core eigenvalues and eigenfunctions were compared with eigenvalues and functions for doubly ionized Mg and 4-times ionized Si. The removal of valence electrons lowered the core eigenvalues by nearly a constant amount and caused small changes in the atomic core functions. These small changes in the core functions are neglected in forming the core-exchange operator. Since the Mg ions in the crystal do not seem to be screened very well by valence electrons, the Mg bare-ion core levels and functions should be unchanged and the Si bare-ion core levels should be raised by about 1 Ry with a small change in the Si core functions. It appears that we would be justified in neglecting the changes to the direct term due to changes in core functions. However, this effect was included.

The SPW expansion of valence functions in the valence-exchange operator is observed to be a good approximation. The normalized valence functions expanded in a truncated series of SPW's required an adjustment of less than 10% in the normalization for all cases. Thus, a small rapidly varying part of the valence functions has been omitted. However, this should not be of serious consequence.

Thus, the HF operator is approximated by

$$H_{\mathrm{HF}} \approx H_{\mathrm{HF}}{}^{\mathrm{BI}} + V + A_{\mathrm{val}}, \tag{22b}$$

where bare-ion core exchange and the dominant valence-exchange components are retained and all direct contributions are included. In Eq. (22b) A_{val} is the valence-exchange operator represented in the approximation described above, and the valence screening potential V includes all contributions to the direct potential that are not already included in $H_{\mathrm{HF}}{}^{\mathrm{BI}}$.

The matrix elements with the bare-ion operator are calculated with the aid of Eq. (20):

$$(\psi_c; H_{\mathrm{HF}}{}^{\mathrm{BI}}\psi_{c'}) = E_c\delta_{cc'}, \tag{23a}$$

$$(\psi_c; H_{\mathrm{HF}}{}^{\mathrm{BI}}\,\mathrm{SOPW},\mathbf{k}) = E_c(\psi_c; \mathrm{SOPW},\mathbf{k}) = 0, \tag{23b}$$

$$\begin{aligned}(\mathrm{SOPW},\mathbf{k}; H_{\mathrm{HF}}{}^{\mathrm{BI}}\,\mathrm{SOPW},\mathbf{k}) &= (\mathrm{SPW},\mathbf{k}; H_{\mathrm{HF}}{}^{\mathrm{BI}}\,\mathrm{SPW},\mathbf{k}') \\ &\quad - \sum_c (\psi_c; \mathrm{SPW},\mathbf{k})^*(\psi_c; \mathrm{SPW},\mathbf{k}')E_c. \end{aligned} \tag{23c}$$

The only term in Eqs. (23) which presents any difficulty is the core-exchange term in Eq. (23c). This term was evaluated by a method described in Appendix B.

The matrix elements with the valence screening potential V were evaluated by expanding V in plane waves. From 100–500 plane waves were used in the expansion. All integrals reduced to Fourier transforms and were evaluated in a straightforward manner. This phase of the calculation was formulated in terms of charge-density matrices which were assembled before the iterative phase of calculation was entered. The calculations proved to be virtually independent of the number (exceeding 4 or 5) of **K**-vector modules that were used in the expansion. The number of terms that were handled in this and succeeding phases of calculation was substantially reduced by symmetry.

In forming the HF operator and in evaluating the matrix elements described above the approximations used were quite good. Such is not the case with the valence-exchange matrix elements. It was a practical necessity to neglect those terms of the matrix elements with the valence-exchange operator which involved core functions. The direct calculation of these terms involves an immense number of difficult integrals. Only the dominant terms have been retained. They have the form

$$\begin{aligned}(\mathrm{SOPW},\mathbf{k}; A_{\mathrm{val}}\,\mathrm{SOPW},\mathbf{k}') &\approx (\mathrm{SPW},\mathbf{k}; A_{\mathrm{val}}\,\mathrm{SPW},\mathbf{k}'), \end{aligned} \tag{24}$$

where the orthogonalization terms have been neglected. This is a serious error and may neglect terms which reduce the exchange matrix elements by as much as 30%. It must be emphasized that although valence functions are well-represented by a truncated plane-wave expansion, the orthogonalization terms in the individual matrix elements need not be small.

The integrals of Eq. (24) are trivial. However, there is a major accounting problem in accumulating them to form the matrix elements. The method which has been used here parallels the HF free-atom matrix methods.[2] First, exchange supermatrices are assembled for each symmetry species and the exchange-matrix elements are then evaluated directly from the supermatrices at each stage of iteration.

3. *A Self-Consistent Procedure*

The first step in the SC procedure is to calculate the eigenfunctions and eigenvalues of the zeroth-order operator $H_{\mathrm{HF}}{}^{\mathrm{BI}}$ for the points in the Brillouin zone corresponding to the translationally inequivalent points in an ECM cell. An improved HF operator is formed in the following way. The plane-wave expansion coefficients of the charge density are calculated from the eigenfunctions for the occupied states. The direct term of the HF operator is calculated from the charge density. At each stage the direct term of the improved HF operator is taken to be the average of the direct term in the preceding stage with the direct term calculated from the charge density.

The valence-exchange operator of the improved HF operator is formed from the most recent valence eigenfunctions for the occupied states. No averaging is done on the exchange operator. The process is discontinued when the changes in the HF operator cause negligible changes in the eigenvalues and direct potential. About five iterations are normally required.

IV. RESULTS FROM THE Mg_2Si CALCULATIONS

SC calculations have been performed for both the Hartree and HF IPM's. The iteration procedure was terminated when the eigenvalues and Fourier coefficients of the direct potential were observed to change by less than 0.002 Ry.

In the first Hartree calculation, the Fourier coefficients of the charge density were obtained for 8 points of the Brillouin zone (a 2×2×2 ECM cell). Essentially the same results were obtained for the Γ, X, and L levels and the SC direct potential when the calculations were extended to a 4×4×4 ECM cell. The 64 points of the Brillouin zone included several points of very low symmetry. We conclude that at least for the direct potential a 2×2×2 ECM cell provides an adequate description of the charge density.

The Hartree calculation was performed as described in the preceding section except that all exchange contributions to the matrix elements were excluded. The results are shown in Fig. 3 where the calculated points are circled. In the Hartree calculations the only approximation of consequence was the Madelung shift approximation. For this reason the sensitivity of the valence and low-lying conduction levels to small shifts of the core energies was studied.

For shifts of all core energies by 0.1 Ry the valence levels were changed by less than 0.01 Ry. The conduction level which was most responsive to the core shifts was the low-lying X_3 level. A shift of 0.1 Ry for the core levels produced a shift in the X_3 level of 0.05 Ry. This sensitivity can be understood as follows.

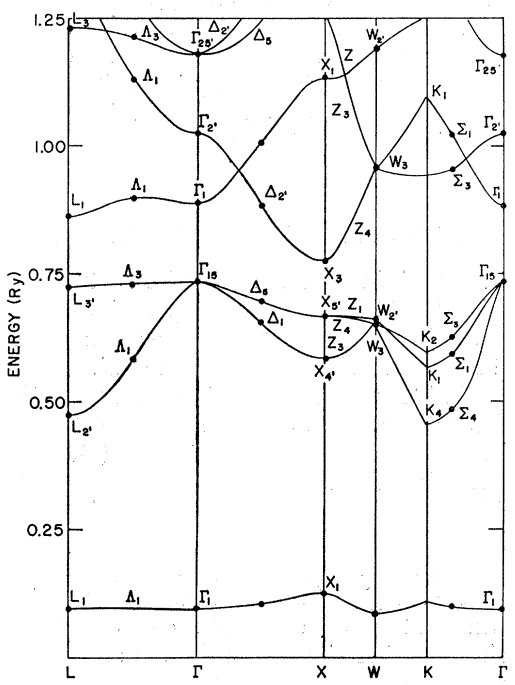

FIG. 3. Hartree energy bands for Mg_2Si. The bands have been subjected to a core shift (0.15 Ry) which brings the indirect gap (0.60 eV) into agreement with experiment. The calculated points are circled and the solid lines indicate compatibility.

TABLE II. Comparison of selected Hartree direct-transition energies with Lee's pseudopotential results (Ref. 21) and the experimental value (Ref. 18).

Direct transition	Calculated energy This work eV	Calculated energy Lee eV	Experiment (Scouler) eV
$X_{5'}$-X_3	1.67	3.9	1.8
Γ_{15}-Γ_1	2.11	3.1	2.1
$L_{3'}$-L_1	2.03	3.2	2.0
$W_{2'}$-W_3	4.1	7.1	3.7–3.9
Σ_3-Σ_3	4.4	?	3.9–4.0
Σ_1-Σ_3	5.0	?	?
$X_{5'}$-X_1	6.3	3.06	?

The core energies enter the valence calculation as a factor on the product of two SOPW orthogonalization coefficients [Eq. (23c)]. If the core energy is low, the SOPW orthogonalization coefficient is small. The largest orthogonalization contribution to the matrix elements is generally from terms involving the highest-core eigenvalues since the product of SOPW orthogonalization coefficients is then relatively large. Thus, a small change in the eigenvalue may produce a significant change in the matrix element. However, to estimate the relative contributions to the matrix elements one must compare s functions with s functions and p functions with p functions. Of course, it is unnecessary to compare functions which are excluded by symmetry. Since the highest-core eigenvalue corresponds to a Mg 2s function, it is not surprising that the X_3 level is sensitive to small shifts in core eigenvalues.

Qualitatively, the Hartree calculations are in complete agreement with the band picture predicted from elementary considerations in Sec. III B. A core shift (0.15 Ry) within the limits prescribed by the Madelung shift approximation brings (a change of 0.05 Ry) the indirect gap (Γ_{15}-X_3) into agreement with experiment. In Table II selected direct transition energies predicted by the adjusted Hartree calculations are listed together with the corresponding results obtained by Lee[21] and the experimental values.[18] The experimental values are assigned on the basis of a critical-point analysis where this is feasible. The first three direct transitions listed predict shoulders in the absorptive part of the dielectric constant ϵ_2 such that for photon energy $\hbar\omega \geq E_d$, the direct-transition energy, $\epsilon_2 \propto (\hbar\omega - E_d)^{1/2}$. Three such shoulders in ϵ_2 can be seen in Scouler's analysis of his Mg_2Si reflectivity data,[18] and this assignment is made with confidence. The calculations also indicate a critical point in the density of states near the direct transition $W_{2'}$-W_3. This seems to be associated with a peak in ϵ_2 at 3.9 eV. We are unable to make a statement about structure observed in ϵ_2 near 3.0 eV. [*Note added in proof.* For technical reasons the Mg_2Si reflectivity data in the

[21] P. M. Lee, Phys. Rev. **135**, A1110 (1964).

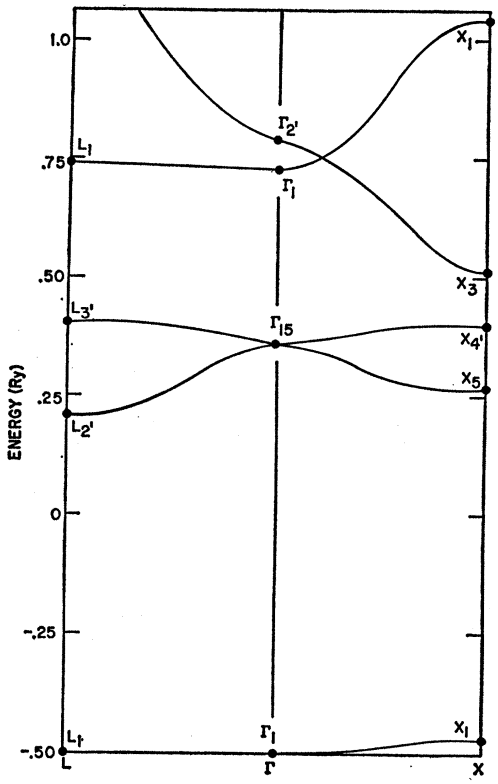

FIG. 4. Energy bands for Mg_2Si based on the HF-IPM. The calculated points are circled and the solid lines indicate compatibility.

region, 1.0–2.5 eV may be unreliable [W. J. Scouler, MIT Lincoln Laboratory, Lexington, Massachusetts, 1967 (private communication)]. A more detailed analysis [Bull. Am. Phys. Soc. **12**, 341 (1967)] based on the Hartree bands indicates that the structure near 3.0 eV is due to transitions along Σ and in the Σ-Λ plane.]

The results of the SC-HF calculations for the 8 points of the Brillouin zone (Γ,X,L) are indicated in Fig. 4. The shape of the low-lying conduction band is qualitatively the same as the corresponding Hartree band. However, the valence bands are significantly different in the HF than in the Hartree calculation. The top of the valence band predicted by HF is at L. Also, the $X_{4'}$ and $X_{5'}$ valence levels have been interchanged.

Since these results are somewhat disconcerting and are probably incorrect, we will reconsider the approximations which were made in forming the HF matrix elements. The sensitivity of the valence and conduction levels to small changes is about the same as discussed for the Hartree calculation. The strange appearance of the valence band is entirely due to the exchange contributions to the matrix elements. If valence exchange is removed, the shape of the HF bands is qualitatively the same as the Hartree bands but the valence band rises into the conduction band. If, as suggested by Phillips and Kleinman's work on Si[4] (and our concern that valence exchange is overestimated), the valence exchange contributions be reduced by a constant factor which is to represent a correlation effect (or crudely account for the neglected terms in the exchange matrix elements), it is possible to remove the strange appearance of the valence band and still have a semiconductor. In doing this the exchange contributions cannot be reduced by more than 30% before the valence band rises into the conduction band, whereas the Si work suggests a reduction of 60–70%.

From the fact that most of the valence-charge density is concentrated near Si sites, it appears likely that the core levels which are most affected by the valence exchange are the Si core levels. An estimate of this effect was made by calculating the valence-exchange contribution to the core eigenvalues in the Si^{-4} ion. This turned out to be a fairly uniform shift of about 0.8 Ry. We might hope that the main effect of the approximations would be to neglect a core shift of the Si core eigenvalues. Such a shift produced almost no change in the shape or position of the bands. Si core shifts are much less critical than Mg core shifts. The Si sites form a tetrahedron centered about a Mg site. Thus, as in the case of Si the valence charge density about a Mg site may be represented by an sp^3 hybrid, but with a much weaker s contribution than is the case for Si. Therefore, we expect the effect of valence exchange on Mg core levels to be much less than on Si core levels and the error to be roughly comparable to the Madelung shift error ($\sim$0.1 Ry).

Thus, an improved treatment of valence exchange will remove the most disturbing feature of the HF bands. However, this is virtually impossible within the present formulation as the terms which have been omitted involve an immense number of difficult integrals.

V. DISCUSSION AND CONCLUSIONS

The ECM is in no sense a radical departure from the traditional HF-IPM. For most purposes it is equivalent. For example, Herman's result for the crystal potential[22] can be obtained simply and directly with the ECM approach. The problem of V_0 has not been solved by the ECM; it has been eliminated along with the difficulties discussed in connection with Eq. (1).

In certain respects the Mg_2Si HF results are comparable to free atom HF results. Certainly, the exchange contributions to the crystal core energies is comparable to the corresponding exchange contributions to the core energies of the constituent atoms or ions. In the case of atoms the exchange-energy contribution to the single-particle eigenvalues for the outermost electrons is a dominant contribution which may determine

[22] F. Herman, in *Proceedings of the Seventh International Conference on the Physics of Semiconductors* (Dunod Cie., Paris, 1964), p. 3.

whether the eigenvalue is negative. In the Mg_2Si calculations neglect of valence-exchange contributions to the single-particle energies caused the valence band to rise into the conduction band. The similarity between free-atom HF results and the Mg_2Si HF results also is apparent in the excitation spectrum of the HF ground-state operator. Excitation spectra of free-atom HF ground-state operators will have the qualitative features (e.g., symmetry of lower-lying excited state vectors) of the observed spectra, but the HF energies of excitation will invariably be too large. The Mg_2Si HF calculations indicate that the exact HF excitation spectrum (excluding the very sensitive X_3 level) will not differ significantly from Fig. 4. Again the similarity between atomic and crystalline HF-IPM's is evidenced by the correct symmetry for the lower-lying excited states, but too large excitation energies.

To our knowledge the only published band calculations in which a serious attempt has been made to include HF exchange are those of Phillips and Kleinman[4] and Brinkman and Goodman[23] on Si. They report that unscreened HF valence exchange completely destroys agreement between their calculated values for the energy gap in Si and the experimental value. Because of the extreme sensitivity of the Mg_2Si gap energy to details in the HF operator we are unable to draw a conclusion about the energy gap. However, the insensitivity of the conduction levels Γ_1 and L_1 to changes in the valence-exchange operator reveals that these levels will be too high even with an exact ECM-HF calculation.

The Mg_2Si HF calculations described in this paper differ from the calculations of Phillips and Kleinman[4] in several respects. The Mg_2Si HF calculations are done self-consistently with a much larger plane-wave basis set than is used in the noniterative Si calculations. In their paper, Phillips and Kleinman list the contributions to matrix elements for the Si $\Gamma_{25'}$ valence level due to valance exchange. It is of interest to note that the self-energy contribution to the matrix element is as large as the remaining terms. This situation does not occur for the Mg_2Si HF calculations because the ECM differs most significantly from the infinite-crystal model in the reduced emphasis on Fourier components of the Coulomb potential with small wave number. To the extent that these small-wave-number components constitute the "long range of the Coulomb interaction" we must conclude that the failure of the ECM version of the HF-IPM to give an excitation spectrum in agreement with experiment to be of the same nature as the corresponding failure in the free-atom HF-IPM.

A pseudopotential band calculation has been performed by Lee[21] on Mg_2Si and Mg_2Ge. In his calculations Lee has superposed the pseudopotentials of Mg and Si and Mg and Ge obtained from independent calculations on the elemental solids in the hope that this approach might lead to reasonable bands for the compounds. The shape of the valence bands calculated by Lee is about the same as the Hartree bands calculated here. However, Lee's conduction bands are significantly different (see Table II) from either of the bands calculated here. At X the conduction levels X_1 and X_3 appear in reversed order. The complete absence of a $\Gamma_{2'}$ conduction level is disturbing in view of the considerations of Sec. III B. A detailed study of the optical and electrical experimental data with the aid of the appropriate selection rules supports the order of levels presented here.[24] In fact, as shown in Table II for direct transitions, the agreement between the Hartree calculation and experiment is remarkable.

[23] W. Brinkman and B. Goodman, Phys. Rev. 149, 597 (1966).

ACKNOWLEDGMENTS

The encouragement and discerning counsel given me by Dr. J. M. Keller throughout the course of this work are deeply appreciated. I wish to thank Dr. F. Herman and Dr. C. C. J. Roothaan for supplying wave functions used in the preliminary stages of this work, Dave Erbeck for programming the atomic calculations, and the staff of the Ames Laboratory Computer Services Group who in various ways have facilitated the extensive computational work. An illuminating conversation with Dr. F. Herman and Dr. B. Goodman is gratefully acknowledged.

APPENDIX A: GENERALIZED LATTICE SUMS

The plane-wave representation of the Coulomb potential

$$\varphi(\mathbf{r})=\sum_{\mathbf{k}\neq 0}(8\pi/k^2\Omega_1)\exp(i\mathbf{k}\cdot\mathbf{r}) \qquad \text{(A1)}$$

cannot be evaluated directly to obtain the potential at a point. This problem was solved by Ewald[25] who was able to rewrite Eq. (A1) as a convergent sum in real space plus a convergent sum in reciprocal space. A simpler derivation due to Ewald and Schockley[26] which emphasizes the physical content of the Ewald method is presented carefully by Slater and DeCicco.[20] The following approach is a generalization of the Ewald scheme.

Let

$$\varphi_{LS}(\mathbf{r})=\sum_{\mathbf{R}^c}\frac{2f^{sr}(a,|\mathbf{r}-\mathbf{R}^c|)}{|\mathbf{r}-\mathbf{R}^c|} \qquad \text{(A2)}$$

be a lattice sum over the appropriate lattice, where $f^{sr}(a,r)$ is a function of the parameter a and the variable

[24] Franco Bassani and Nathan O. Folland, J. Phys. Chem. Solids (to be published).

[25] P. P. Ewald, Ann. Physik 64, 253 (1921).

[26] See, e.g., C. Kittel, *Introduction to Solid State Physics* (John Wiley & Sons, Inc., New York, 1956), 2nd ed., p. 571.

TABLE III. Generalized lattice sum parameters.

$f^{sr}(a,r)$	$\Omega_1 C(a,\mathbf{k})$	$\Omega_1 C(a,\mathbf{0})$
$\operatorname{erfc}(ar)$	$(8\pi/k^2)\exp(-k^2/4a^2)$	$-2\pi/a^2$
$\exp(-ar)$	$8\pi a^2/k^2(a^2+k^2)$	$-8\pi/a^2$

r. The only requirement that is placed on f^{sr} is that the plane-wave expansion

$$\varphi_{LS}(\mathbf{r})=\sum_{\mathbf{k}} c(a,\mathbf{k})\exp(i\mathbf{k}\cdot\mathbf{r}) \tag{A3}$$

exists and converges. The plane-wave expansion coefficients are

$$c(a,\mathbf{k})=\Omega_1^{-1}\int \exp(-i\mathbf{k}\cdot\mathbf{x})2f^{sr}(a,x)x^{-1}d\mathbf{x}. \tag{A4}$$

Consider the identity

$$\varphi(\mathbf{r})=\varphi_{LS}(\mathbf{r})+(\varphi(\mathbf{r})-\varphi_{LS}(\mathbf{r})). \tag{A5}$$

By substituting Eqs. (A1) and (A3) for φ and φ_{LS} in the bracketed term in the right member of Eq. (A5), we obtain an expression in the form of an Ewald lattice sum,

$$\varphi(\mathbf{r})=\varphi_{LS}(\mathbf{r})+C(a,\mathbf{0})+\sum_{\mathbf{k}\neq\mathbf{0}} C(a,\mathbf{k})\exp(i\mathbf{k}\cdot\mathbf{r}), \tag{A6a}$$

where

$$C(a,\mathbf{0})=-\operatorname*{limit}_{\mathbf{k}\to\mathbf{0}} c(a,\mathbf{k}) \tag{A6b}$$

and

$$C(a,\mathbf{k})=(8\pi/k^2\Omega_1)-c(a,\mathbf{k}). \tag{A6c}$$

The Ewald result is recovered if we choose

$$f^{sr}(a,r)=\operatorname{erfc}(ar)=(4/\pi)^{1/2}\int_{ar}^{\infty}\exp(-t^2)dt.$$

The usefulness of a particular form of Eqs. (A6) depends on the application for which it is intended. The efficacy of the Ewald method for calculating a periodic potential at a point is not questioned. In Table III are listed the relevant parameters for two choices of simple analytic functions f^{sr} for which the convergence of both series in Eq. (A6) is improved appreciably over that of the original series [Eq. (A1)]. Evidently there are very few simple functions which have this desirable property.

By construction the potential in the form of Eq. (A6) is independent of the parameter a. The two examples listed in Table III have the property that for large values of the parameter a the potential approaches the form of Eq. (A1).

APPENDIX B: CORE EXCHANGE WITH PLANE WAVES

Matrix elements of the core-exchange operator [Eq. (16)] with plane waves have the form,

$$(\mathrm{PW},\mathbf{k};A_{\mathrm{core}}\,\mathrm{PW},\mathbf{k}')=\Omega_0^{-1}\sum_{js}\exp(i(\mathbf{k}-\mathbf{k}')\cdot\mathbf{R}_s)$$
$$\times\int \exp(-i\mathbf{k}\cdot\mathbf{r}_1)\phi_{js}^*(2)H_{12}$$
$$\times\exp(i\mathbf{k}'\cdot\mathbf{r}_2)\phi_{js}(1)d\mathbf{r}_1d\mathbf{r}_2. \tag{B1}$$

Since the core functions ϕ_{js} are tightly bound, we may replace H_{12} by $2/r_{12}$. Let

$$F(\mathbf{k})=\int \exp(i\mathbf{k}\cdot\mathbf{r})\phi(\mathbf{r})d\mathbf{r}, \tag{B2}$$

where we drop the subscripts from the core functions. Then, with the aid of the identity

$$1/r_{12}=2(2\pi)^{-2}\int d\mathbf{x}\,x^{-2}\exp(i\mathbf{x}\cdot\mathbf{r}_{12}), \tag{B3}$$

a typical term of Eq. (B1) becomes

$$I=2(2\pi)^{-2}\int d\mathbf{x}\,x^{-2}F^*(\mathbf{k}-\mathbf{x})F(\mathbf{k}'-\mathbf{x}). \tag{B4}$$

The Fourier transforms of the core functions were approximated by linear combinations of Gaussians

$$F(\mathbf{k})=\sum_m (4\pi)^{1/2}Q_m(k^2)\exp(-b_mk^2)\begin{pmatrix}1\\ \mathbf{k}\end{pmatrix}, \tag{B5}$$

where $Q_m(k^2)$ is a polynomial in k^2. Since F may be either an s or a p function in $\mathbf{k}$ space, both possibilities are included in the bracketed factor in Eq. (B5). The Fourier transforms were approximated by a least-squares technique in which both exponents and coefficients were varied until no further decrease in the average least-squares deviation occurred. Although it was especially difficult to approximate the high-Fourier components for the more tightly bound core functions, it was felt that a good approximation had been obtained for all core functions.

In terms of Eq. (B5)

$$I=\sum_{m,m'}(2/\pi)\int d\mathbf{x}\,x^{-2}\exp[-b_m(\mathbf{k}-\mathbf{x})^2$$
$$-b_{m'}(\mathbf{k}'-\mathbf{x})^2]Q_m((\mathbf{k}-\mathbf{x})^2)Q_{m'}((\mathbf{k}'-\mathbf{x})^2)$$
$$\times\begin{pmatrix}1\\ 3(\mathbf{k}-\mathbf{x})\cdot(\mathbf{k}'-\mathbf{x})\end{pmatrix}. \tag{B6}$$

Equation (B6) may be rewritten as

$$I=\sum_{m,m'}Q_m(-\partial/\partial b_m)Q_{m'}(-\partial/\partial b_{m'})$$
$$\times\exp(-b_mk^2-b_{m'}k'^2)$$
$$\times\begin{pmatrix}1\\ 3[\mathbf{k}\cdot\mathbf{k}'-\frac{1}{2}(\partial/\partial b_m+\partial/\partial b_{m'})]\end{pmatrix}I', \tag{B7a}$$

where

$$I'=(2/\pi)\int d\mathbf{x}\, x^{-2}\exp(-bx^2+2\mathbf{x}\cdot\mathbf{K}), \quad \text{(B7b)}$$

with $b=b_m+b_{m'}$ and $\mathbf{K}=b_m\mathbf{k}+b_{m'}\mathbf{k}'$. Equation (B7b) becomes, after several transformations,

$$I'=4(\pi/b)^{1/2}\int_0^1 \exp(K^2t^2/b)dt, \quad \text{(B8a)}$$

which is related to the confluent hypergeometric function

$$I'=4(\pi/b)^{1/2}\,{}_1F_1(\tfrac{1}{2};\tfrac{3}{2};K^2/b). \quad \text{(B8b)}$$

Since the integral, Eq. (B8a), is evaluated a large number of times in the course of a calculation of core-exchange matrix elements with plane waves, it was necessary to develop high-speed methods for determining its value. By tabulating the function and interpolating the value of the function by a central-difference technique we were able to reduce the calculation time (on an IBM 7074) to a maximum of 0.5 msec per integral. Fortunately, we were able to compare our calculated values to a table of the function prepared by Lohmander.[27] The calculated points compared to 8 digits and the interpolated points to 4 digits. Thus, we expect an accuracy of about 2–3 significant digits in the core-exchange matrix elements with plane waves.

Since the derivatives in Eq. (B7) make the equations more complicated, the least-squares technique was biased to keep the power of the polynomials as small as possible.

An accurate method for calculating core-valence exchange integrals where core functions are represented by linear combinations of Slater functions has been described recently by Brinkman and Goodman.[22]

[27] B. Lohmander and S. Rittsen, Kgl. Fysiograf. Sallskap. Lund, Forh. 28, 45 (1958).

PHYSICAL REVIEW VOLUME 158, NUMBER 3 15 JUNE 1967

Shubnikov–de Haas Effect in $SrTiO_3$†

H. P. R. Frederikse, W. R. Hosler, and W. R. Thurber
National Bureau of Standards, Washington, D. C.

AND

J. Babiskin and P. G. Siebenmann
U. S. Naval Research Laboratory, Washington, D. C.

(Received 23 January 1967)

The magnetoresistance of semiconducting $SrTiO_3$ has been investigated in high magnetic fields (up to 150 kOe). In the temperature range 1.4–2.1°K, for fields of more than 50 kOe, well-developed Shubnikov–de Haas-type oscillations have been observed. The data support a conduction band consisting of spheroids along the ⟨100⟩ crystalline axes, having 3 minima at the points X_3. The periods of oscillation as well as the temperature dependence of the amplitude and the magnetic field saturation lead to the following values for the transverse and longitudinal effective masses: $m_t=1.5m_0\pm15\%$; $m_l=6.0m_0\pm30\%$.

INTRODUCTION

THE observation of quantum effects in the electronic properties of metals and semiconductors has been and is being used extensively to probe the energy-band structure of such solids. Cyclotron resonance, oscillatory susceptibility (de Haas–van Alphen effect) and oscillatory magnetoresistance (Shubnikov–de Haas effect) are the three most popular phenomena being investigated.

Considering the interest in the electronic properties of $SrTiO_3$, the question arose whether these experiments could be applied fruitfully to the further exploration of its band structure. A promising theoretical calculation of the electronic energy scheme[1] exists, and a majority of relevant experiments[2–7] seems to confirm this band picture. However, no direct measurement of the tensor elements of the effective mass has been attempted thus far. The application of the magnetic quantum effects to a material like $SrTiO_3$ poses con-

† Research supported in part by the National Aeronautics and Space Agency.

[1] A. H. Kahn and A. J. Leyendecker, Phys. Rev. 135, A1321 (1964).
[2] H. P. R. Frederikse, W. R. Thurber, and W. R. Hosler, Phys. Rev. 134, A442 (1964).
[3] A. S. Barker, in *Proceedings of the International Colloquium on Optical Properties and Electronic Structures of Metals and Alloys, Paris, 1965* (North-Holland Publishing Company, Amsterdam, 1965).
[4] Manuel Cardona, Phys. Rev. 140, 651 (1965).
[5] H. P. R. Frederikse, W. R. Hosler, and W. R. Thurber, Phys. Rev. 143, 648 (1966).
[6] H. P. R. Frederikse and G. A. Candela, Phys. Rev. 147, 583 (1966).
[7] O. N. Tufte and E. L. Stelzer, Phys. Rev. 141, 675 (1966).